

Tuomas Mennola, Mikko Mikkola, Matti Nojonen, Tero Hottinen and Peter Lund, Measurement of ohmic voltage losses in individual cells of a PEMFC stack, Journal of Power Sources 112 (1) 2002, pp. 261-272.

© 2002 Elsevier Science

Reprinted with permission from Elsevier.

## Measurement of ohmic voltage losses in individual cells of a PEMFC stack

Tuomas Mennola<sup>\*</sup>, Mikko Mikkola, Matti Noponen, Tero Hottinen, Peter Lund

*Laboratory of Advanced Energy Systems, Helsinki University of Technology, P.O. Box 2200, FIN-02015 HUT, Espoo, Finland*

Received 12 February 2002; received in revised form 12 July 2002; accepted 15 July 2002

### Abstract

The ohmic voltage loss in a fuel cell can be determined with the current interruption method. The method was utilized to measure the ohmic voltage loss in an individual cell of a fuel cell stack. This was achieved by producing voltage transients and monitoring them with a digital oscilloscope connected in parallel with the individual cell. In this study, the method was applied to a small polymer electrolyte membrane fuel cell (PEMFC) stack in which different air supply levels were employed on the cathode side. In the case of higher air-feed rate, the results revealed an increase of ohmic losses in the middle of the stack by up to 21% at  $400 \text{ mA cm}^{-2}$ , compared to the unit cell with the lowest ohmic loss. This probably resulted from the decrease of membrane conductivity because of drying. Comparison to individual cell voltages showed that the decrease of conductivity would not be observed if only the individual cell voltages alone were measured. The total ohmic loss in the stack was measured using the same method to verify the reliability of the measurement system. The results indicate a good agreement between the total ohmic loss and the combined ohmic losses in the individual cells.

© 2002 Elsevier Science B.V. All rights reserved.

*Keywords:* Current interruption; Ohmic loss; PEMFC; Stack

### 1. Introduction

The polymer electrolyte membrane fuel cell (PEMFC) technology is rapidly advancing towards commercialization in many applications ranging from portable power sources to transportation applications and distributed power generation. For the development of application-ready stacks, new measurement methods are needed for fast characterization and diagnostics. The performance of individual cells in a stack needs to be understood in order to optimize the stack design and the operating conditions.

In a stack, the cells are electrically connected in series and the polarization curves of individual cells can be measured by measuring the current of the entire stack and the voltages of individual cells. The polarization behavior of a fuel cell results from three types of phenomena: electrode kinetics, ohmic losses, and transport limitations. To understand the operation of the cell and to determine the performance limiting factors, the contributions of different overpotentials need to be identified. In this study, we focus on the measurement of ohmic losses.

The largest single source of ohmic losses in a PEMFC is the proton conductive membrane, which acts as the electrolyte and gas separator. The conductivity of common organic membrane materials is strongly dependent on the hydration state of the membrane. Therefore, the measurement of ohmic losses gives important information on water management, which in turn is a critical issue for the successful operation of a PEMFC. Water management is influenced by several parameters including current density, cell temperature, and the flow rate and humidity of the reactant gases. The construction of a stack brings up additional challenges, since there may be significant variation in temperature and mass transfer conditions in different parts of a stack.

An increase of ohmic losses may also be an indication of the poisoning of the membrane by various impurities. For example, ions originating from metallic parts of the cell may contaminate the membrane, reducing its conductivity.

Ohmic losses also arise from the resistance of the electrically conductive components and the contact resistances at their interfaces. Excessive ohmic losses may therefore be an indication of high contact resistances resulting from the surface oxidation of the components or the improper assembling of the stack.

In this work, we employed the current interruption method to measure the ohmic losses in individual cells of a small stack.

<sup>\*</sup> Corresponding author. Tel.: +358-9-451-3217; fax: +358-9-451-3195.  
E-mail address: tmennola@cc.hut.fi (T. Mennola).

Two different air supply methods were used during the measurements, resulting in different water management conditions. We begin with a discussion on the basic principles of the current interruption method and the description of our measurement systems. The measurements are described and analyzed, and their accuracy and reliability is discussed.

## 2. Current interruption method

The two in situ methods that are commonly employed for measuring the ohmic loss in electrochemical cells are the current interruption method [1,2] and ac impedance spectroscopy [3–5]. In the current interruption method, the ohmic part of the overpotentials is separated from the electrochemical losses by taking advantage of the fact that the ohmic losses vanish faster than the electrochemical overpotentials when the current is interrupted. In ac impedance spectroscopy, the response of the studied system to ac signals is analyzed by fitting data from simultaneous phase and amplitude measurements either to an equivalent circuit model of the system or to a model described by partial differential equations.

The current interruption method is commonly used in single cell studies, and it can also be used to measure the total ohmic loss in a stack. However, the authors are not aware of any published studies on the application of this, or any other method, to the measurement of the ohmic loss in an individual cell of a stack.

The basic principle of the current interruption method is to interrupt the current and to observe the resulting voltage transient. The ideal shape of a voltage transient after a current interruption is depicted in Fig. 1. The potential drop

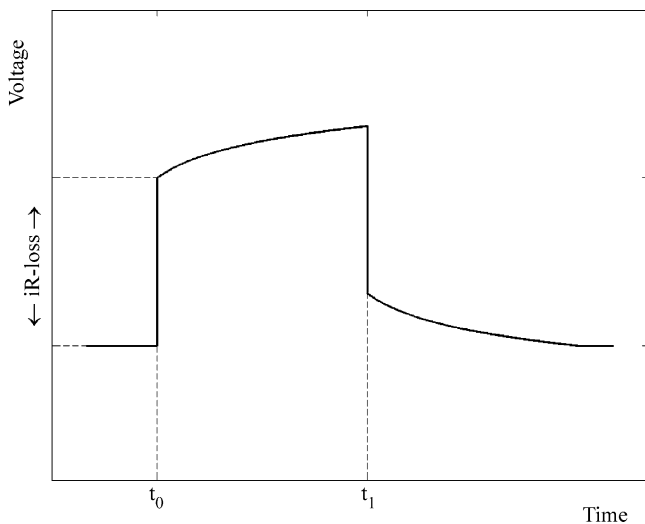


Fig. 1. An ideal voltage transient in a fuel cell after a current interruption. The cell is operated at a fixed current. At  $t = t_0$ , the current is interrupted and the ohmic losses vanish almost immediately. After the current interruption, electrochemical overpotentials start to decay and the voltage rises exponentially towards the open-circuit voltage. At  $t = t_1$ , the current is again switched on.

caused by ohmic resistance vanishes almost immediately, whereas the relaxation of electrochemical overpotentials takes place at a considerably slower rate. Therefore, the ohmic loss can ideally be measured from the difference between the voltage immediately before and after the current interruption. Thus, compared to impedance spectroscopy, the current interruption method has the advantage of more straightforward data analysis.

The current interruption method can also be implemented by superimposing auxiliary current pulses to the cell current through a separate circuit [6,7]. The current pulse method has the advantage of producing faster and cleaner current decays, especially when the cell current is high.

In practice, voltage transients recorded from fuel cells exhibit features not appearing in the idealized curve in Fig. 1. After the current interruption, a voltage overshoot takes place, followed by oscillations. The same kinds of effects are also observed in reverse when the current is switched on again. These effects result from the inductance of the measurement circuitry. Therefore, they become worse when the size of the load circuitry is increased. In addition to the inductance-related effects, the data also contains noise from the measurement electronics.

Because of the non-ideal features appearing in the recorded voltage transients, the determination of the ohmic loss from the data requires some consideration. A straightforward method is to define the ohmic loss as the difference between the voltage recorded immediately before the interruption and the voltage recorded shortly after it. In this case, the accuracy of the method is dependent on the adjustment of the delay between the current interruption and the measurement of the voltage.

If the  $iR$ -free voltage is measured too early, the reading may be affected by the overshoot and the oscillations occurring immediately after the interruption. On the other hand, measuring it too late leads to the systematic overestimation of the ohmic loss, because some relaxation of the electrochemical overpotentials has already taken place, as can be seen from Fig. 1. It is also possible that some decaying of the electrochemical losses takes place already before the oscillations have fully subsided. Therefore, the accuracy of the results may be improved by extrapolating the rising voltage curve back to the actual moment of interruption.

In order to choose the appropriate methods for the analysis of the measurements, an essential question is to find estimates for the rates of the slowest electrical processes and the fastest electrochemical processes. An estimate for the relaxation rate of ohmic losses has been presented by Büchi et al. [6]. By considering the dielectric relaxation times of the ionic and electronic conductors in the cell, they concluded that ohmic losses decrease to less than 1% of the initial value in approximately half a nanosecond after the current interruption.

There are no published studies on how to determine by theoretical considerations the time scale of the fastest electrochemical reactions occurring in a PEMFC. In [6], an

experimentally derived time scale of 10 ns was used for the fastest electrochemical reactions. Based on these estimates, the ideal time window for measuring the ohmic loss would be 0.5–10 ns after the current interruption. If this time window is masked by the non-idealities of the measurement system, extrapolation should be performed in order to improve the accuracy of the results.

### 3. Measurements

#### 3.1. Measurement system and fuel cell

A CompuCell<sup>®</sup> Fuel Cell Test Station GT-100, made by GlobeTech Inc., was used in the measurements. The Fuel-Cell software by Scribner Associates Inc., running on a PC, performed the tasks of system control, measurement automation, and data logging. Individual cell voltages were measured with a separate data logging system.

The load unit of the test station features a built-in current interrupter circuitry for measuring the total ohmic loss in the cell or stack under test. It operates continuously, taking a measurement approximately once per second. The system processes the data internally and provides the final ohmic loss reading to the user.

The measurement of the ohmic loss in an individual cell of a stack can be achieved by monitoring the current interruptions with a fast voltage-sampling device connected in parallel with the cell under measurement. The use of a continuous voltage-sampling device also makes it possible to evaluate the quality of the data and to perform extrapolations if needed. Our first experiments with this method have been reported in [8].

A Tektronix TDS-320 digital oscilloscope with a 10X passive probe was used to record the current interruptions. The input impedance of the oscilloscope is 1 M $\Omega$ . The data recorded by the oscilloscope was transferred via GPIB to a computer for processing and analysis.

Because only the difference between the operating voltage and the *iR*-free voltage is interesting, the oscilloscope was set to the ac coupled mode, in which the dc component of the signal is removed. The use of the ac mode removes the need to constantly adjust the trigger level to compensate for short-term fluctuations in the cell voltage. This made it easier to achieve stable triggering especially at low current densities, where the ohmic loss was small. In order to further stabilize the triggering, the high-frequency rejection mode of the oscilloscope was used. The high-frequency rejection mode attenuates frequencies above 30 kHz. This was found to reduce false triggering that results from the noise of the system, especially at low current densities.

A commercial four-cell stack was used in this study. The active area of each cell was 25 cm<sup>2</sup>. The cathode sides of the bipolar plates had straight vertical channels, and the ends of the channels were open to the ambient air. The open-cathode structure makes it possible to operate the stack either on free

convection or with a small fan feeding the air. Open-cathode stacks are therefore well suited for small applications.

When a fan was used, it was placed under the stack to produce an upward airflow. The fan was installed in a cardboard housing, which served as a support structure and directed the airflow to the inlets of the stack. Because the diameter of the fan was slightly larger than the length of the stack, it also caused some air to flow along the endplates of the stack, providing external cooling. The fan was powered by an external power supply at a constant power of 1.2 W with no adjustments for current density. The fan system was a later modification and not an original part of the stack.

#### 3.2. Operating conditions

Dry hydrogen was used as fuel. The hydrogen stoichiometry was set to 1.5, using the mass flow controller of the test station to control the flow rate. Because ambient air was used on the cathode, the humidity of air could not be controlled, but it was monitored using a Vaisala HMI41 relative humidity and temperature indicator with a HMP42 probe. Ambient temperature was 22 °C and relative humidity approximately 20% during the measurements.

The stack was operated on both free and forced convection. When free convection was used, the ohmic losses in individual cells were measured at current density levels of 100, 150 and 200 mA cm<sup>-2</sup>. The use of forced convection made it possible to obtain higher current densities. The current levels were extended from 100 to 400 mA cm<sup>-2</sup> in steps of 50 mA cm<sup>-2</sup>. The improved performance results both from more effective water removal and from higher oxygen concentration in the air channels. At high current densities, free convection is unable to supply enough oxygen to the reaction sites, resulting in an uneven current density distribution [9].

No external heating was used during the measurements. This approach was chosen because we wanted to investigate the variation of ohmic losses arising as a result of the intrinsic temperature distribution of the stack. If external heating had been used, the temperature distribution would have been affected by the heating elements.

#### 3.3. Measurement practices

When the measurements were performed, the stack was first allowed to reach a stable operating temperature at each current density level. The temperature was considered stable when it had remained within  $\pm 0.5$  °C for at least 10 min. The temperature of the stack was measured with a thermocouple sensor, which was inserted into the flow-field plate at the cathode end of the stack.

At each current density level, a sequence of voltage transient measurements was performed. A voltage transient was first recorded for the whole stack. Then the individual cells were measured one by one, and finally another measurement for the whole stack was performed in order to

check for possible changes in the state of the stack. During the measurement sequence, the total voltage and temperature of the stack, and the voltage of each cell were recorded. If the temperature of the stack changed from the beginning of the sequence by more than one degree, the data was discarded and the sequence was repeated.

The probe tip and ground connectors of the oscilloscope were connected directly to the flow-field plates of the individual cell being measured. The probe tip was connected to the cathode side flow-field plate and probe ground lead was connected to the anode side flow-field plate. When the ohmic loss in the entire stack was measured, the probes were also connected to the flow-field plates. Thus, the contributions of the current leads and the end plates of the stack were not included in the readings.

The duration of measurement sequences was kept to the minimum in order to ensure that the state of the stack would remain as unchanged as possible. At each step, the trigger level was adjusted, one transient was recorded as soon as stable triggering was achieved, and the data was transferred to the PC. The typical duration of a measurement sequence was approximately 3 min.

The amount of electronic noise in the readings could have been reduced by recording several transients in succession and averaging them. However, this would have increased the duration of the measurement sequence. Therefore, in order to keep the changes in the state of the stack to the minimum, only single transients were recorded for each individual cell and whole-stack measurement.

As a practical observation, it was noticed that if the stack being measured is connected to the electrical ground, it is important to isolate the oscilloscope from the ground with an isolating transformer. Otherwise, the operation of the stack will be disturbed when the oscilloscope probes are connected to it. In addition, the computer used to transfer data from the

oscilloscope needs to be isolated from the ground, since one of the leads of a GPIB cable provides a ground connection.

## 4. Results

### 4.1. Overview of the data

Examples of the recorded transients, representing typical features, are depicted in Figs. 2–5 for the free convection case and in Figs. 8–11 for the forced convection case. As expected, the transients feature a significant overshoot immediately after the interruption. The duration of the overshoot was approximately 3–4  $\mu\text{s}$ , which clearly exceeds the estimated relaxation time of the ohmic losses. Therefore, the main concern in the analysis of the data is to avoid interpreting the fastest electrochemical processes as ohmic loss. Based on the estimate for the time scale of the fastest electrochemical processes, it appears that extrapolation should be performed to obtain the  $iR$ -free voltage.

The data contains significant amounts of electronic noise, which in the individual cell measurements at low current densities is almost of the same magnitude as the ohmic loss itself. However, this is not a serious problem for the practical use of this method, since when the ohmic loss is small, it is generally less interesting to measure it with high precision.

In order to determine the real voltage levels from the noisy data, line fitting was performed using the MathCad software by MathSoft Inc. For the determination of the initial voltage level, a straight line was fitted into the data from the last 20  $\mu\text{s}$  before the interruption. Another straight line was fitted into the data from the first 20  $\mu\text{s}$  after the end of the overshoot. A fixed interval of 4  $\mu\text{s}$  was used between the end of the first line fitting region and the beginning of the second line fitting region.

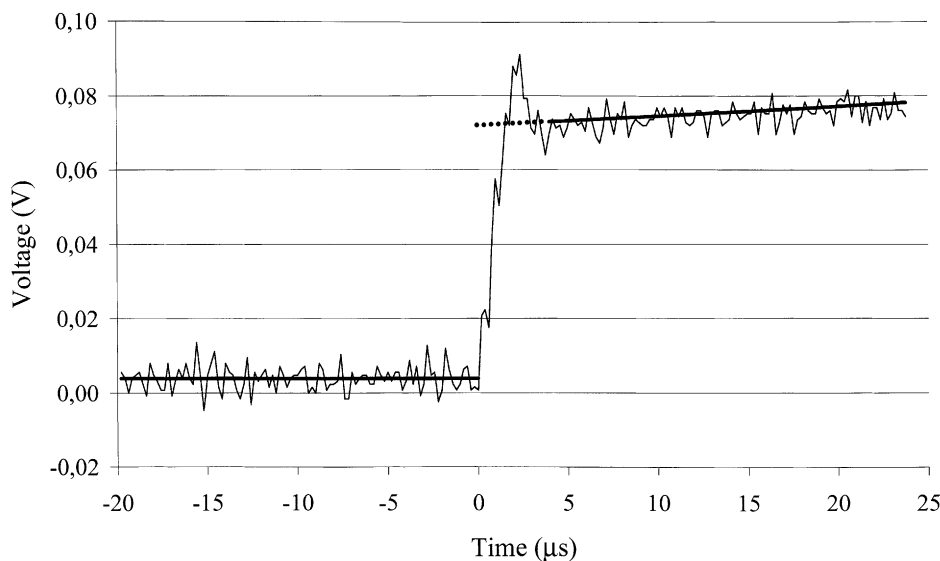


Fig. 2. Voltage transient (thin line) and fitted average voltage (bold line) for the whole stack. Extrapolation is indicated with a dotted line. Air supply: free convection;  $j = 100 \text{ mA cm}^{-2}$ .

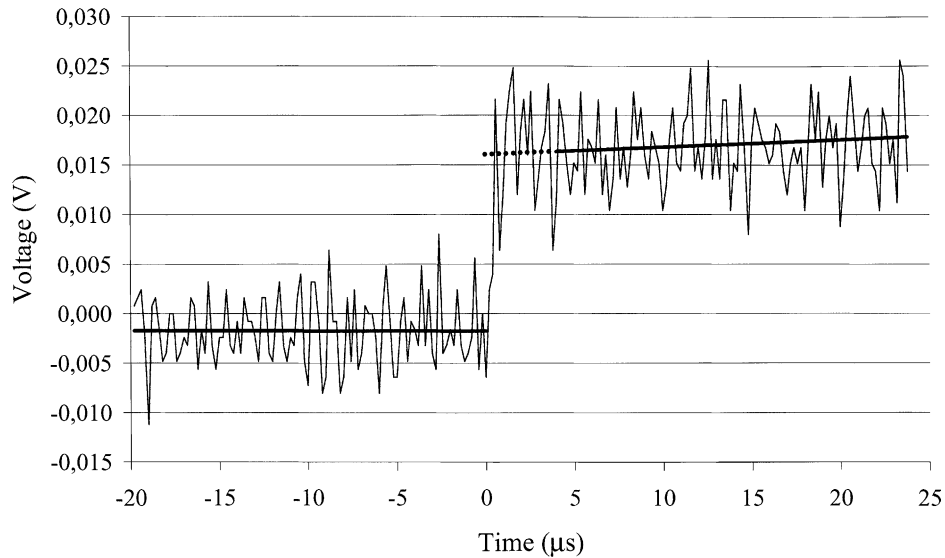


Fig. 3. Voltage transient (thin line) and fitted average voltage (bold line) for an individual cell. Extrapolation is indicated with a dotted line. Air supply: free convection;  $j = 100 \text{ mA cm}^{-2}$ .

The relaxation of the electrochemical overpotentials is generally a non-linear process. More accurate results might be obtained by fitting an exponential curve into the data as suggested, e.g. in [6]. However, the noise in the data makes it difficult to ascertain, whether the data contains true indications of exponentially decaying processes. The shape of the voltage behavior immediately after the overshoot might be interpreted as the relaxation of electrochemical overpotentials. The possible exponential shape is best visible in the whole-stack transients. However, it could also be interpreted as oscillating behavior that follows the overshoot. In addition, the possible exponential part of the curve is relatively short and does not contain a very large number

of data points to produce a good fitting. Therefore, it was decided to use a linear fitting in all cases in order to obtain consistent results.

The ohmic loss was finally calculated using the fitted lines. The end of the fitting region before the interruption was adjusted to coincide with the actual moment of interruption. The line, which was fitted to the region after the interruption, was extrapolated to the same point of time. The ohmic loss was then determined from the difference between the fitted lines at this point of time.

In the next sections, the results are discussed in detail. Due to the volume of the data, some representative examples of the transients are depicted and the rest of the data is

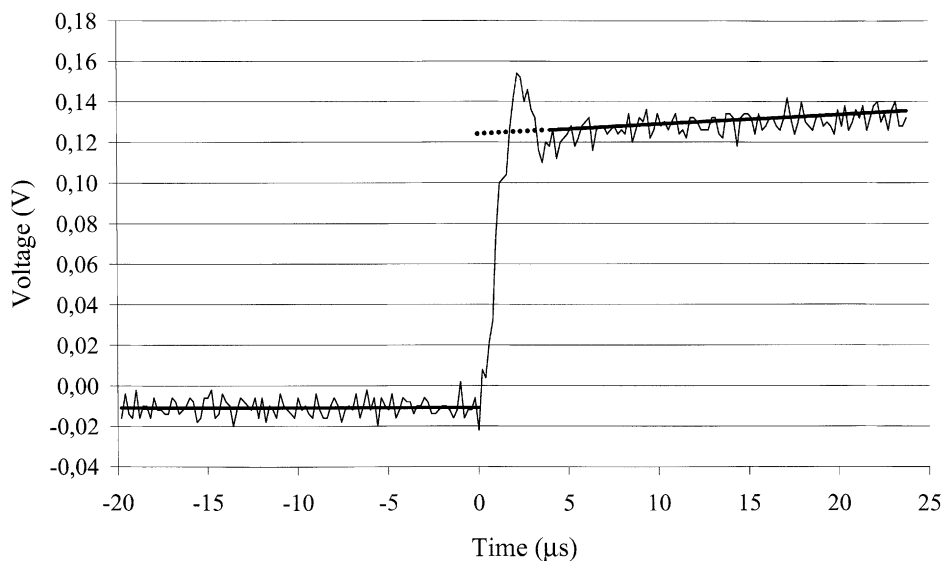


Fig. 4. Voltage transient (thin line) and fitted average voltage (bold line) for the whole stack. Extrapolation is indicated with a dotted line. Air supply: free convection;  $j = 200 \text{ mA cm}^{-2}$ .

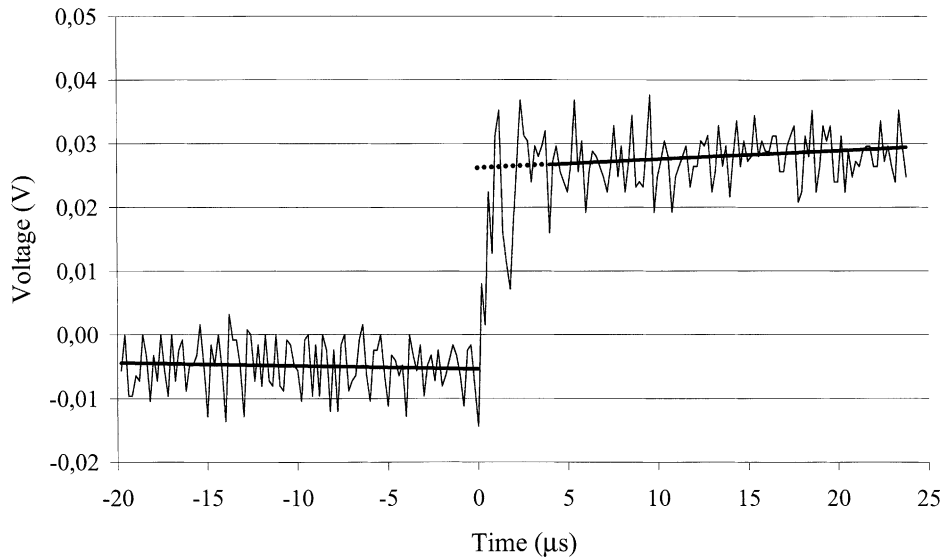


Fig. 5. Voltage transient (thin line) and fitted average voltage (bold line) for an individual cell. Extrapolation is indicated with a dotted line. Air supply: free convection;  $j = 200 \text{ mA cm}^{-2}$ .

summarized by plotting the calculated ohmic losses. For both free and forced convection, the transients recorded at the highest and lowest of the current density levels are depicted. At each current density level, the first of the whole-stack transients and the transient in individual cell 1 are shown. The individual cells were numbered starting from the anode end of the stack.

#### 4.2. Free convection

In the free convection case, the measurement sequences were performed at three current density levels. The voltage transients recorded for the whole stack and an individual cell

at the lowest current density ( $100 \text{ mA cm}^{-2}$ ) are depicted in Figs. 2 and 3. The respective transients recorded at the highest current density ( $200 \text{ mA cm}^{-2}$ ) are depicted in Figs. 4 and 5. The calculated ohmic losses are depicted in Fig. 6.

The strongest peaks of electronic noise deviated approximately 10 mV from the average voltage levels. In the individual cell measurements, noise was therefore quite significant compared to the actual ohmic loss, which was 16–18 mV per cell at the lowest current density. The effect of noise became smaller when the current density was increased. In the whole-stack measurements, the ohmic loss was higher and the effect of noise accordingly smaller.

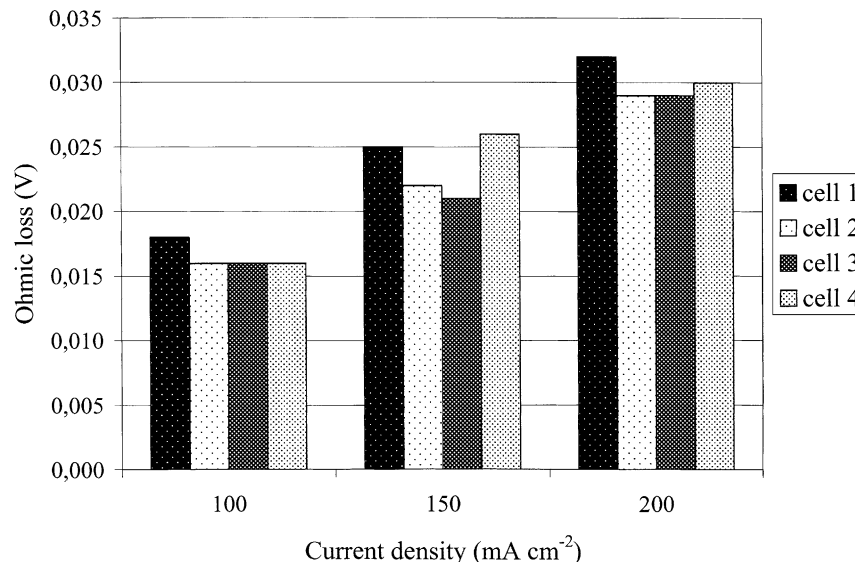


Fig. 6. Measured ohmic losses in individual cells. Air supply: free convection.

There appears to be some consistency in the variation of ohmic losses across the stack as the current density increases, as it can be seen in Fig. 6. The consistency of the results can be taken as an indication of reasonably good reliability. However, the largest differences are only 5 mV and therefore some caution must be exercised in the interpretation of the results.

Based on the results, it appears that the cells in the center had the lowest ohmic losses. The center cells probably reached a slightly higher temperature than the end cells, resulting in a higher conductivity, and lower ohmic losses, in the center cell membranes. The conductivity of common membrane materials is normally improved with rising temperature as long as hydration of the membrane remains constant. The assumption of full hydration is probably true, since liquid water was observed in the air channels during the measurements in all of the unit cells. However, the differences in the ohmic losses might be attributed to other factors, such as differences in the contact resistances between the cell components, or uncertainties in the extrapolation procedure.

The individual cell voltages recorded during the voltage transient measurements are depicted in Fig. 7. The difference between the highest and lowest of the cell voltages is 86 mV at 100 mA cm<sup>-2</sup> and 82 mV at 200 mA cm<sup>-2</sup>. The variation of individual cell voltages is considerably larger than the variation of ohmic losses. The variation of voltages must therefore be primarily due to other factors. The fact that the variation of voltages is significant already at the lowest current density might indicate that activation overpotentials are the main reason for the differences.

The stack temperatures during the voltage transient measurements are listed in Table 1. Because the stack was not actively cooled, there was a significant increase of temperature from 100 to 200 mA cm<sup>-2</sup>.

Table 1  
Stack temperatures during the measurement of ohmic losses<sup>a</sup>

Current density (mA cm <sup>-2</sup> )	Temperature (°C)
100	38
150	45
200	51

<sup>a</sup> Air supply: free convection.

#### 4.3. Forced convection

In the forced convection case, the measurement sequences were performed at seven current density levels. The voltage transients recorded for the whole stack and an individual cell at the lowest current density (100 mA cm<sup>-2</sup>) are depicted in Figs. 8 and 9. The respective transients recorded at the highest current density (400 mA cm<sup>-2</sup>) are depicted in Figs. 10 and 11. The calculated ohmic losses are depicted in Fig. 12.

Comparison to the free convection case reveals that the ohmic losses were higher as a result of increased water removal. Visual observation of the stack confirmed that little or no liquid water was present in the air channels. Therefore, it appears possible that some drying was taking place. At 200 mA cm<sup>-2</sup>, the ohmic losses were 47–49 mV per cell. On free convection, they were 29–32 mV per cell at the same current density. The noise level and the general quality of the data were similar to the free convection case.

The pattern of the variation of ohmic losses across the stack appears to have changed quite notably from the free convection case. As the current density increases, the ohmic losses appear to increase faster in the middle cells than in the end cells. At 100 mA cm<sup>-2</sup>, the cells 2 and 3 had the lowest ohmic losses. However, at 400 mA cm<sup>-2</sup>, the ohmic loss in

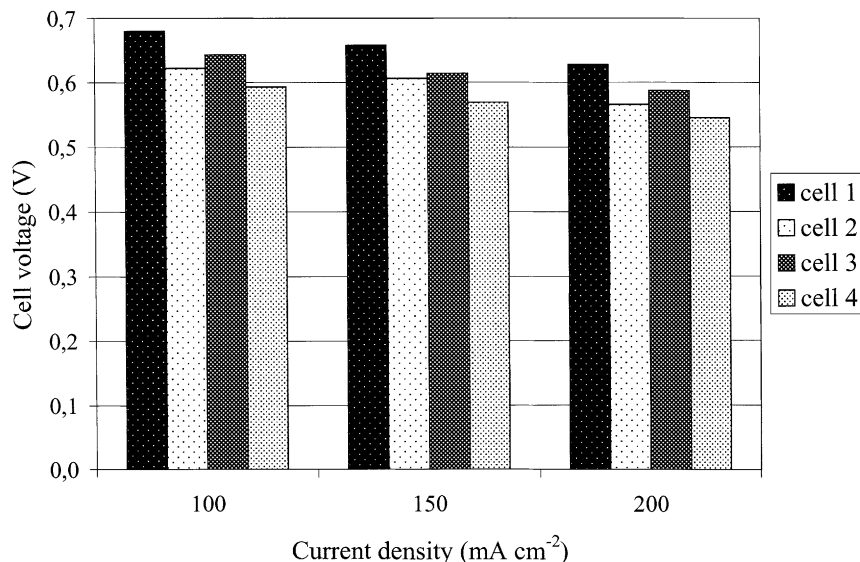


Fig. 7. Individual cell voltages during the measurement of ohmic losses. Air supply: free convection.

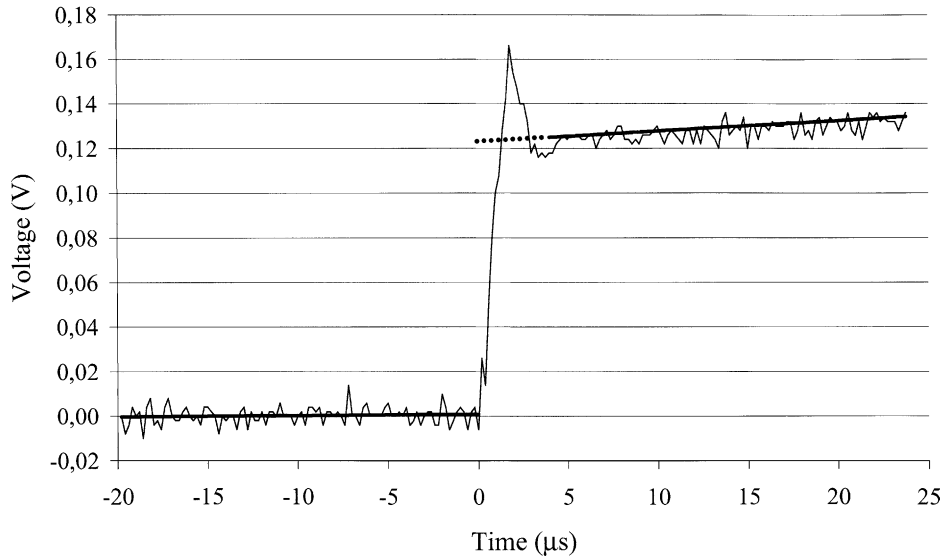


Fig. 8. Voltage transient (thin line) and fitted average voltage (bold line) for the whole stack. Extrapolation is indicated with a dotted line. Air supply: forced convection;  $j = 100 \text{ mA cm}^{-2}$ .

cell 3 was 17 mV (21%) higher than in cell 1, which had the lowest ohmic loss at this current density. The most likely explanation is that the temperature distribution inside the stack became more uneven at high current densities, the center cells being at higher temperature than the end cells. This resulted in slightly more severe dehydration of the membranes in the center cells compared to the end cells. The air flow rate, which was higher than in the free convection case, also contributed to the drying. This explains why the same effect was not observed in the free convection case, despite the generally higher temperature levels.

It might also be hypothesized that the drying of the middle cells might be the result of an uneven distribution of airflow between the cells. The fan was carefully positioned under the stack, with the aim of feeding air at an equal rate to every cell, but no attempts were made to directly measure the flow rates in individual cells. However, the apparent drying effect became more pronounced at high current densities. On the other hand, the air stoichiometry was decreasing with increasing current density, since the fan was operated at a constant power. Therefore, an excessive airflow alone does not explain the observed drying.

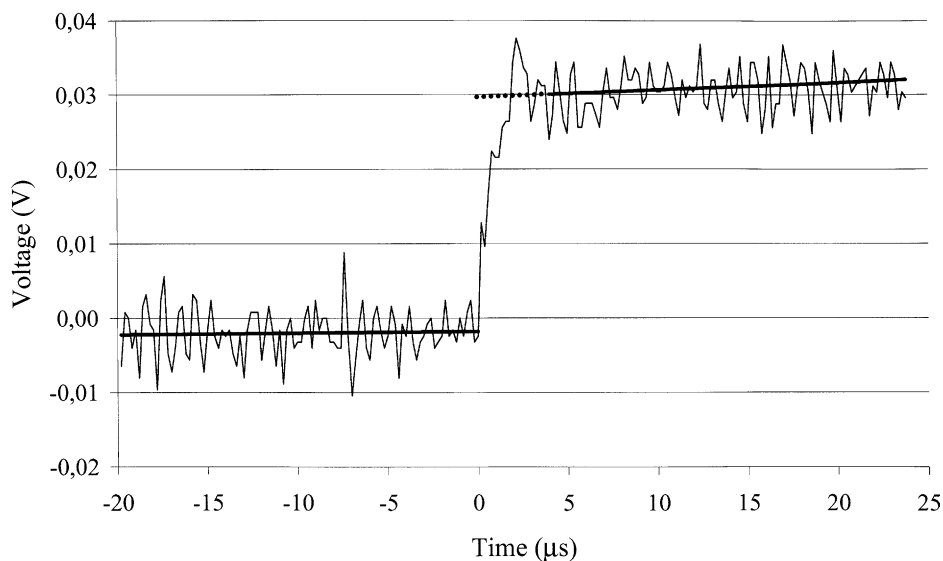


Fig. 9. Voltage transient (thin line) and fitted average voltage (bold line) for an individual cell. Extrapolation is indicated with a dotted line. Air supply: forced convection;  $j = 100 \text{ mA cm}^{-2}$ .

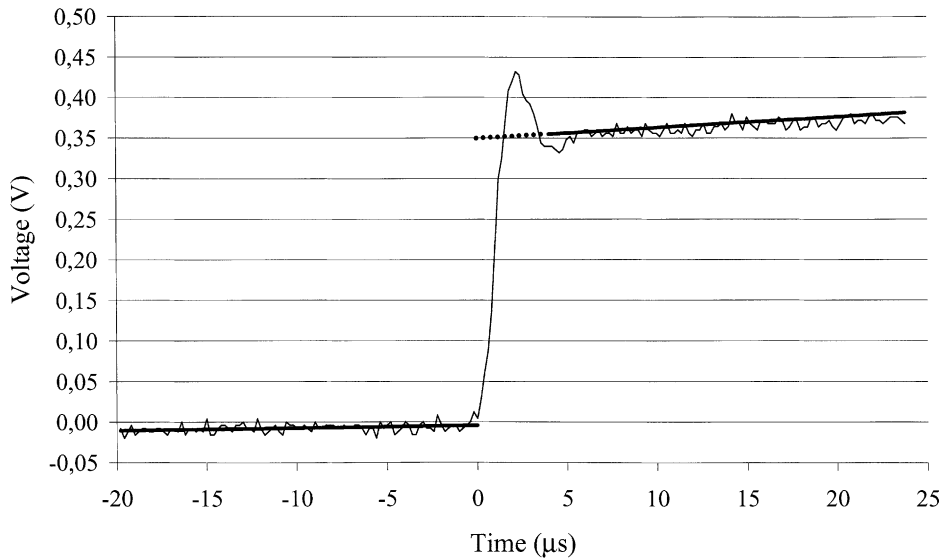


Fig. 10. Voltage transient (thin line) and fitted average voltage (bold line) for the whole stack. Extrapolation is indicated with a dotted line. Air supply: forced convection;  $j = 400 \text{ mA cm}^{-2}$ .

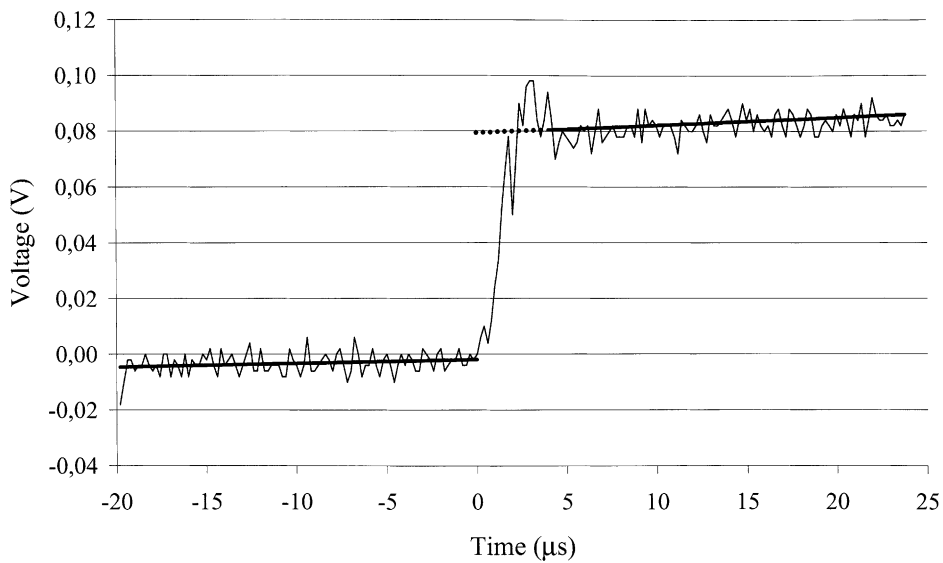


Fig. 11. Voltage transient (thin line) and fitted average voltage (bold line) for an individual cell. Extrapolation is indicated with a dotted line. Air supply: forced convection;  $j = 400 \text{ mA cm}^{-2}$ .

The individual cell voltages recorded during the voltage transient measurements are depicted in Fig. 13. The pattern of variation is quite similar to what it was on free convection. Again, the comparison between ohmic losses and cell voltages confirms that the variation of cell voltages was mostly due to electrochemical losses. The difference between the highest and lowest of the cell voltages is 102 mV at  $100 \text{ mA cm}^{-2}$  and 128 mV at  $400 \text{ mA cm}^{-2}$ .

The stack temperatures during the voltage transient measurements are listed in Table 2. Because the increased airflow had a cooling effect, the temperature of the stack

Table 2  
Stack temperatures during the measurement of ohmic losses<sup>a</sup>

Current density ( $\text{mA cm}^{-2}$ )	Temperature ( $^{\circ}\text{C}$ )
100	27
150	29
200	31
250	33
300	35
350	37
400	39

<sup>a</sup> Air supply: forced convection.

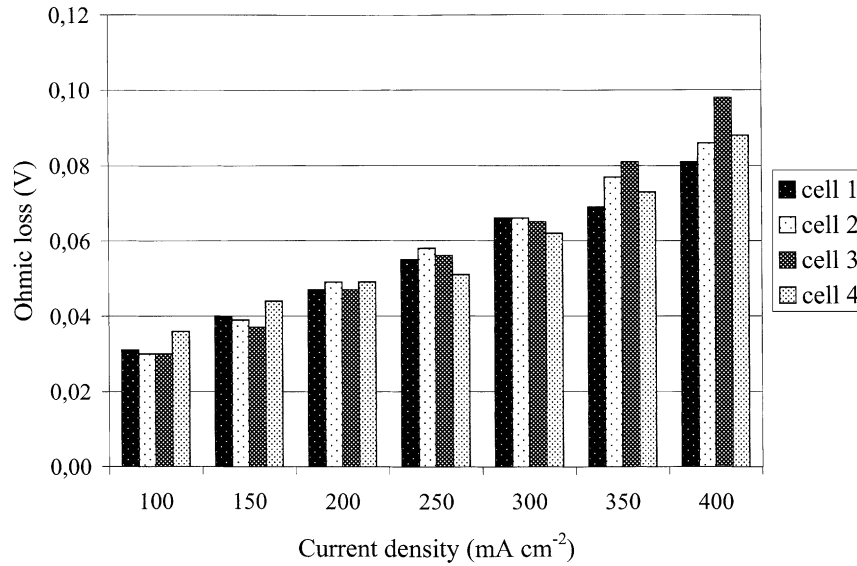


Fig. 12. Measured ohmic losses in individual cells. Air supply: forced convection.

remained considerably lower than in the free convection case.

4.4. Total ohmic loss in the stack

Additional insights into the reliability of the measurement system can be gained when the sum of the ohmic losses in individual cells in each case is compared to the ohmic loss measured across the whole stack. The whole-stack measurement was performed before and after the sequence of individual cell measurements. The comparisons in free and forced convection cases are depicted in Figs. 14 and 15, respectively.

The results indicate good agreement between the sum of individual cell readings and the whole-stack readings. No systematic differences can be observed. In the case of forced convection, it is interesting to note that the curve representing the sum of individual cells actually has a more steadily rising shape than the whole-stack curves, in which random scatter appears to be higher. One possible interpretation is that when the measured voltage transient is larger, also the overshoot and oscillations are more pronounced and therefore extrapolation uncertainties are increased, resulting in increased scatter in the data.

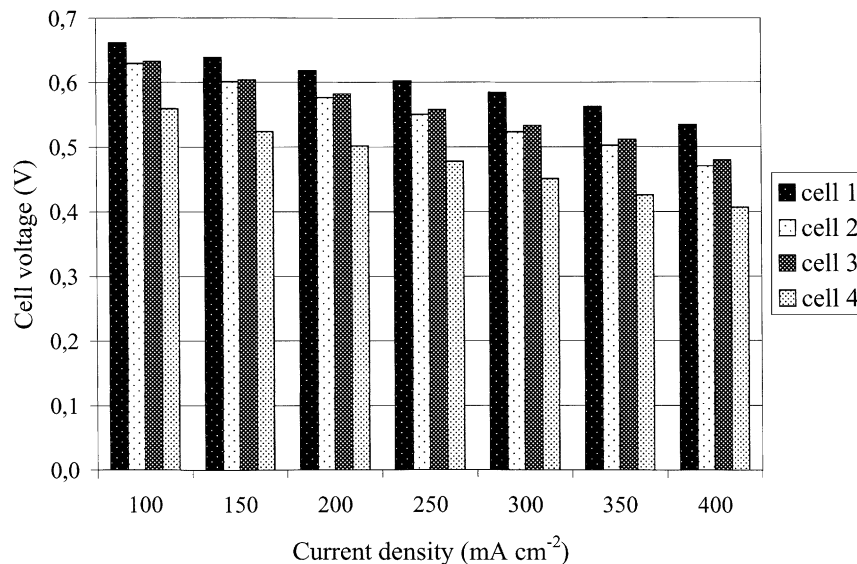


Fig. 13. Individual cell voltages during the measurement of ohmic losses. Air supply: forced convection.

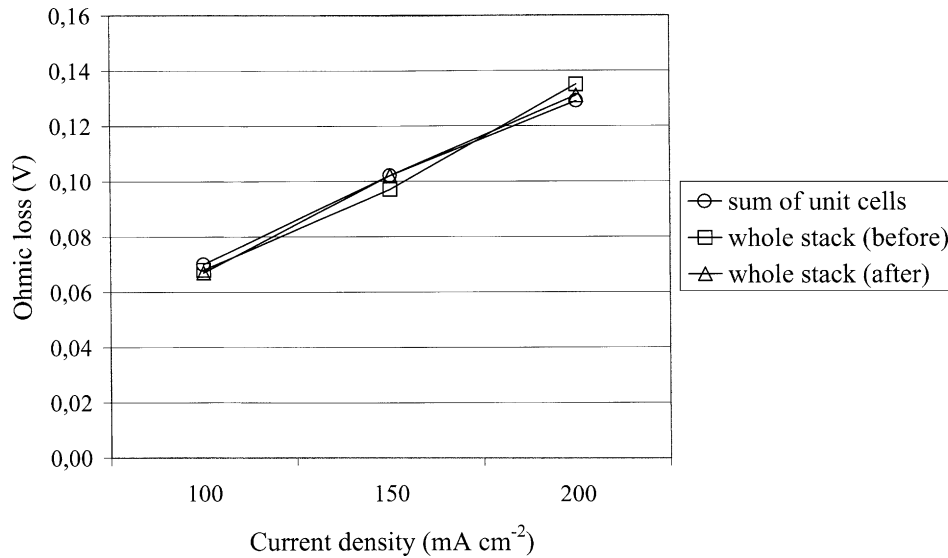


Fig. 14. Comparison of the combined ohmic losses in the unit cells to the ohmic loss in the whole stack before and after the unit cell measurements. Air supply: free convection.

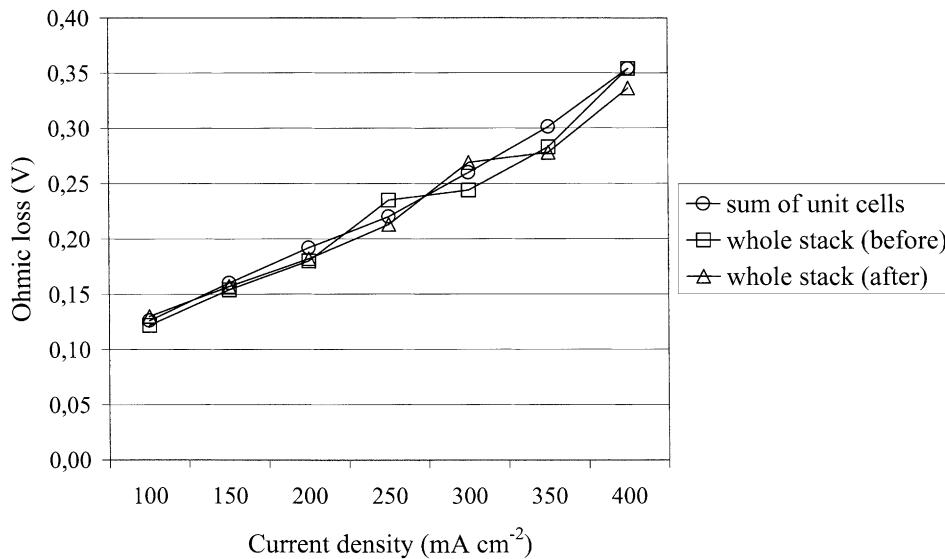


Fig. 15. Comparison of the combined ohmic losses in the unit cells to the ohmic loss in the whole stack before and after the unit cell measurements. Air supply: forced convection.

## 5. Conclusions

In this work, we have studied the application of the current interruption method to the measurement of the ohmic losses in the individual cells of a fuel cell stack. This was achieved by employing a digital oscilloscope to continuously record the individual cell voltages while performing current interruptions. The stack was not modified in any way for the measurements. The current interruption method provides valuable diagnostic information about the performance of a stack, since it makes it possible to separate the contribution of ohmic losses from other overpotentials. Monitoring only the cell voltages of a stack does reveal which cells are

performing weakly, but it does not reveal the source of the problem. When a method is available to measure the ohmic losses in individual cells, the need for guesswork is reduced when stack problems are diagnosed and opportunities for performance improvements are sought.

During the measurements, the stack was operated using two different air supply methods. On free convection, no reduction of conductivity with increasing current density was observed, which indicates that the cell remained well humidified. The ohmic losses in individual cells were found to be very close to each other, which clearly indicates that the observed differences in the cell voltages were due to other overpotentials.

When a small fan was used to feed air into the cathode channels of the stack, considerably higher current densities could be obtained. However, a slight increase of ohmic losses was observed, especially in the cells in the middle of the stack at high current densities. This effect would have gone unnoticed, if the performance of the stack was monitored only by measuring the individual cell voltages. The increase of ohmic losses was probably due to overheating, which resulted in the drying of the membranes. Heat production takes place within the thin electrode regions, and therefore, local overheating problems may not always be easily diagnosed by direct temperature measurements, unless the temperature sensors are placed very close to the electrodes. The measurement of ohmic losses provides an alternative method to reveal possible heat transfer problems without modifying the stack.

Possible sources of error that might affect the results include changes in the state of the stack during the measurement sequences and errors resulting from the extrapolation procedure used in the determination of the ohmic loss. The sum of the ohmic losses in individual cells was compared to the total ohmic loss in the stack, measured with the same method. Good agreement was found, indicating that the state of the stack had remained essentially unchanged. Therefore, the largest single source of error was probably the extrapolation procedure, since it is likely that some decay of the

electrochemical overpotentials was hidden behind the overshoot after the current interruption.

### Acknowledgements

The financial support of the National Technology Agency of Finland (Tekes) is gratefully acknowledged.

### References

- [1] W.J. Wruck, R.M. Machado, T.W. Chapman, *J. Electrochem. Soc.* 134 (1987) 539–546.
- [2] C. Lagergren, G. Lindbergh, D. Simonsson, *J. Electrochem. Soc.* 142 (1995) 787–797.
- [3] J.R. Selman, Y.P. Lin, *Electrochim. Acta* 38 (1993) 2063–2073.
- [4] T.E. Springer, T.A. Zawodzinski, M.S. Wilson, S. Gottesfeld, *J. Electrochem. Soc.* 143 (1996) 587–599.
- [5] M. Ciureanu, H. Wang, *J. Electrochem. Soc.* 146 (1999) 4031–4040.
- [6] F.N. Büchi, A. Marek, G. Scherer, *J. Electrochem. Soc.* 142 (1995) 1895–1901.
- [7] F.N. Büchi, G.G. Scherer, *J. Electroanal. Chem.* 404 (1996) 37–43.
- [8] M. Mikkola, Master's Thesis, Helsinki University of Technology, Espoo, 2001.
- [9] M. Noponen, T. Mennola, M. Mikkola, T. Hottinen, P. Lund, *J. Power Sources* 106 (2002) 304–312.